

We are IntechOpen, the world's leading publisher of Open Access books Built by scientists, for scientists

4,800

Open access books available

122,000

International authors and editors

135M

Downloads

Our authors are among the

154

Countries delivered to

TOP 1%

most cited scientists

12.2%

Contributors from top 500 universities



WEB OF SCIENCE™

Selection of our books indexed in the Book Citation Index
in Web of Science™ Core Collection (BKCI)

Interested in publishing with us?
Contact book.department@intechopen.com

Numbers displayed above are based on latest data collected.
For more information visit www.intechopen.com



Nanofluids and Computational Applications in Medicine and Biology

Laith Jaafer Habeeb and Hasan Shakir Majdi

Abstract

The chapter comprises of two sections: the first concerns with the nanofluids, and the second is about the computational applications in medicine and biology. Nanotechnology is a novel logical methodology that includes materials and gear equipped for controlling the physical just as chemical properties of a substance at subatomic dimensions. This innovation can possibly expel the evident limits between biology, physics, and chemistry to some degree and shape up our present thoughts and comprehension. Consequently, numerous new difficulties and bearings may likewise emerge in education, research, and diagnostics in parallel by the extensive use of nanobiotechnology with the progression of time. Blood flow modeling in various arteries is an important topic of CFD biomechanics. Regardless of these endeavors and advances, there are as yet confounded inquiries around, for example, the interaction between blood flow and various artery diseases.

Keywords: nanofluidics, computational fluid dynamics, fluid-structure interaction, multiphysics systems coupling, multiphase flow

1. Introduction

The use of solid particles, like particles having millimeter or micrometer size, as additives suspended into the base fluid has been well recognized for numerous years. Nevertheless, they have not been of attention for the practical uses owing to problems, like the sedimentation that leads to increase the pressure drop in the channel of flow. The recent progress in the technology of material has done it able to engender an innovative nanofluid via the suspension of the particles having nanometer size in the base fluids that can vary the fluid movement and some properties of the base fluid. The nanofluids are solid-liquid composite alloys comprising solid nanofibers or nanoparticles having sizes distinctively from 1 to 100 nm suspended in a fluid. Various base fluids are commonly used. These are water, organic liquids (e.g., ethylene, triethylene glycols, refrigerants, etc.), oils and lubricants, bio-fluids, and polymeric solutions. The nanoparticles utilized in nanofluids include chemically stable metals (gold, copper, aluminum), metal oxides (alumina, silica, zirconia, and titania), metal carbides (SiC), metal nitrides (AlN, SiN), various forms of carbon (diamond, graphite, carbon nanotubes, fullerene), and functionalized nanoparticles. It is not a simple liquid-solid blend; the highly significant criterion of nanofluid is the agglomeration of freely steady suspension

for long periods without resulting in any chemical variations in the base fluid. That can be done via increasing the liquid viscosity, via preventing the particles from agglomeration, and via using particles having nanometer size. The particle settling can prevent or minimize the density between solids and liquids [1].

Classical science and engineering disciplines already provide a wide, well-established base of knowledge for the understanding of these phenomena of nanofluids. Examples of areas that deal intensively with nanoscale phenomena include tribology, surface sciences, and colloid sciences (**Figure 1**).

Another classical research field that previously dealt with nanofluidic phenomena is the surface science, which studies the phenomena occurring at the interface of two phases, such as solid-liquid interfaces, solid-gas interfaces, and liquid-gas interfaces (**Figure 2**).

Computational fluid dynamics (CFD) is the using of computer-based simulation to analyze the systems that involve fluid flow, heat transfer, and connected phenomena. A numerical model is initially built utilizing a set of mathematical equations describing the flow. Then, such equations are solved employing a computer program for obtaining the flow parameters within the domain of flow. The development and application of CFD have undergone a considerable growth, and as a result, it has become a powerful tool in the design and analysis of engineering and other processes [2]. The governing equations of the models are partial differential equations (PDEs). Because the digital computers can merely recognize and handle the numerical data, such equations cannot be solved straightforward. Thus, the partial differential equations must be converted into numerical equations including merely the numbers and no derivatives. Such operation of making a numerical analogue to the partial differential equations is named “numerical discretization.” The discretization operation includes an error because the “numerical” terms are merely the approximations to the initial “partial differential” terms. Such error, nevertheless, can be much reduced to low and thus acceptable levels. The main

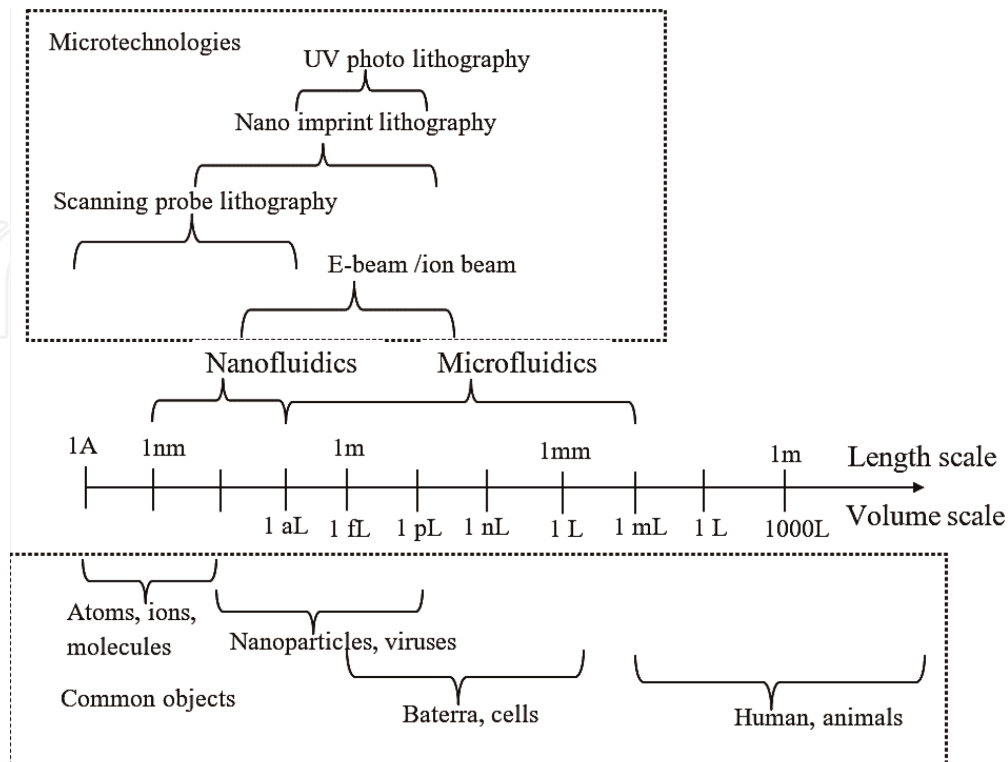


Figure 1. Length scales and volume scales of nanofluidics, microfluidics, common microtechnologies, and common objects [1].

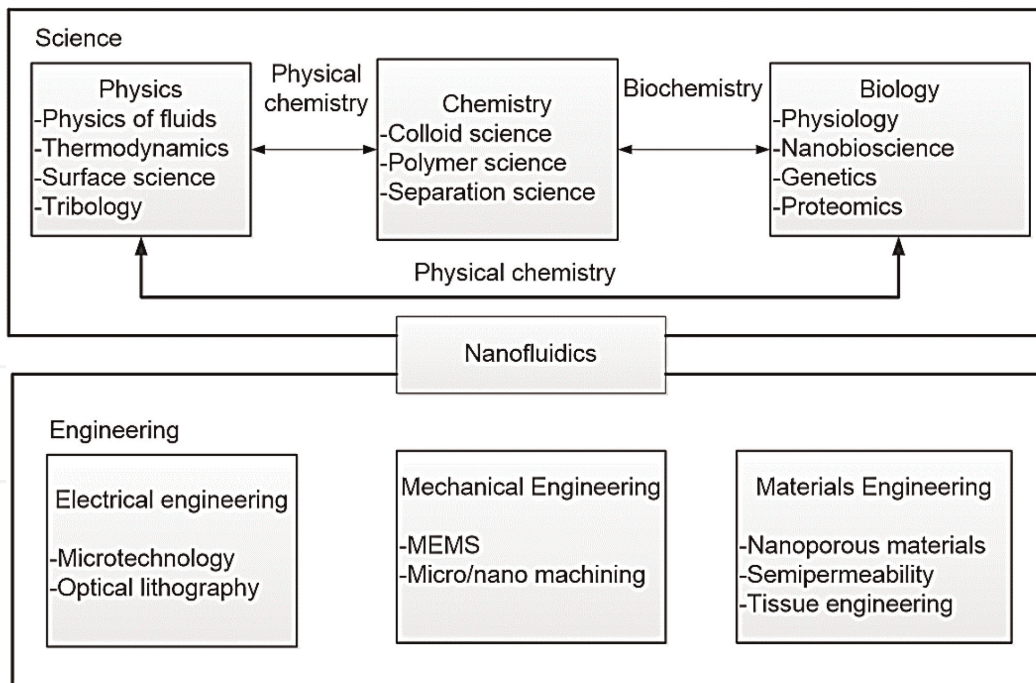


Figure 2.
 Classical areas of science and engineering related to nanofluidics [1].

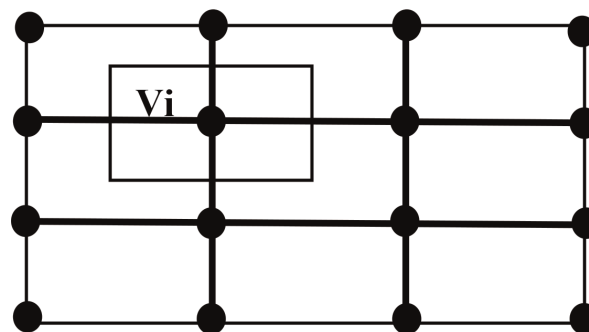


Figure 3.
 A control volume (V_i) surrounded by mesh elements.

technique utilized for discretization is the “finite volume method.” This method is likely the highly famous one employed for the “numerical discretization” in CFD. In some ways, it’s similar to the “finite difference method (FEM),” but certain of its tools drag the features taken from the FEM. Such method includes discretization of spatial domain into the finite control volumes. The control volume overlaps with numerous mesh elements, and thus it can be split into sectors, each one backs to various mesh elements, as depicted in **Figure 3**.

The governing differential equations are integrated over every control volume. The obtained laws of integral conservation are precisely met for every control volume and for the whole domain, which is a discrete benefit of the FEM. Then, every integral term is changed into a separate form, therefore providing discretized equations at the nodal points, or centroids, of control volumes.

2. Some advantages and applications of using nanofluid and CFD

Due to the size of nanoparticles, the pressure drop is minimal, and a strong change in the properties of the main fluid, by the suspension of nanofluids and because of the size of nanoparticles, the liquid is considered one fluid.

According to the application, nanofluids are classified as heat transfer nanofluids, environmental (pollution cleaning) nanofluids, bio- and pharmaceutical nanofluids, and medical nanofluids (drug delivery, functional and tissue-cell interaction) [3]. The biomedical industry, for instant, the conventional method of cancer treatment kill the cells of cancers, drugs the radiation without damaging, cool the brain, and safe the surgery. Nanofluids can be utilized for cooling the equipment of welding and engines of automobiles and for cooling the high heat flux instrument, like a high-power laser diode array and high-power microwave tubes. Nanofluid can move throughout the tiny passage in MEMS to enhance efficiency. Within the industry of transportation, nanocars, General Motors (GM), are used. The nanofluid critical heat flux (CHF) measurement in a forced convection loop is beneficial for the nuclear uses. If nanofluid enhances the efficiency of the chiller by 1%, an electricity saving of 320 billion KWh or equivalent 5.5 million barrel of oil annually would be released in the USA only. Nanofluids possess the capability for the operations of deep drilling. Also, the nanofluid can be utilized to increase the dielectric power and age of an oil transformer via spreading nanodiamond particles [1].

There are numerous practical engineering problems for which one cannot determine the exact solutions. Such incapability to determine a perfect solution may be ascribed to either the intricate nature of the governing differential equations or the difficulties that accrue from treating with the boundary and primary conditions. To treat with these problems, one resorts to numerical approximations. In contrast to the analytical solutions, which reveal the perfect behavior of a regime at any point through it, the numerical solutions approximate the perfect solutions merely at separate points. Two- and three-dimensional (CFD) modeling is time-consuming and computationally more expensive than one-dimensional analytical modeling. However, it can provide more information of the flow. It is also an effective alternative to experimental investigation. The simulation setup can be changed more flexibly than the experimental setup. Where is CFD used? It is used in aerospace, automotive, biomedical and chemical processing, HVAC (heating, ventilation, and air conditioning), hydraulics, marine, oil and gas, power generation, sports, etc. The major kinds of the fluid flow problems that the general-purpose CFD codes can solve are:

- a. Kinds of flow: transient or steady, viscous or inviscid, laminar or turbulent (using a variety of turbulent models such as the k-model), compressible or incompressible, subsonic or supersonic speeds, or ultrasonic, multiphase (continuous phases or particles), chemical reacting, combustion, swirling, and non-Newtonian
- b. Heat transfer modes: conduction, convection, and radiation
- c. Kinds of material: solid (porous or homogenous) and fluid (gas or liquid)
- d. Kinds of coordinate systems: cylindrical polar, Cartesian, curvilinear, moving/rotating, and body fitted

The use of computers is to help with all phases of engineering design work. Like computer-aided design (CAD), but also involving the construction and analysis of objects, the idea is to use computer processing and interactive computer graphics to enable engineers to create, modify, and analyze designs and hence to determine the structural, thermal, flow-field properties or other conditions of a regime. Computer-aided engineering (CAE) programs may employ a geometry definition

from a CAD program as a starting point and always use some forms of FEA as the tool to conduct the analysis. The advantages of CAE system are:

- a. It is capable of carrying out different engineering analyses, such as stresses and deformations, buckling, contact analyses, plastic deformations, vibration, heat transfer, fluid flow, magnetic field, coupled field problems, design optimization, etc.
- b. It can work interactively with the CAD systems.
- c. The analyses are facilitated through GUI (graphical user interface).
- d. Different types of material properties can be included: isotropic, orthotropic, nonlinear, etc., and there is reduction of time.
- e. Analysis and simulation can be modified and revised easily.
- f. The results are presented graphically.

The disadvantages of CAE system are high cost of CAE software and special and advanced hardware, optical fatigue, and high cost of user's training and qualification.

3. Selected topics in nanofluidics and computational applications

Computational fluid dynamics studies are performed to grow a deeper insight into the field of the flow. In order to clarify the influence of the turbulence model, which involves the solution of a two-transport equation, model is used. Therefore, the techniques of the numerical solution will solve these Cartesian coordinate systems (x , y , and z). A three-dimensional geometry will generate.

3.1 Preparation of nanofluid and calculation of the thermal conductivity

Nanoparticles are made in one of two ways: physical processes and chemical processes. The physical techniques include mechanical grinding and the inert gas condensation technique. The chemical processes include chemical precipitation, spray pyrolysis, and thermal spaying. There are two ways to prepare nanofluid [1].

3.1.1 Single-step method

Single-step technique combines the production of nanoparticles and dispersion of nanoparticles into base fluid in a single step by the aid of chemical solvents [4].

3.1.2 Two-step method

This is the most widely used method for preparing nanofluids. This gives a large-scale production of nanofluids, whereas the single-step method is limited, in which dry powders are dispersed into a fluid. The second step is processing with the help of intensive magnetic force agitation, high-shear mixing, ultrasonic agitation, ball milling and homogenizing [4].

The main drawback in the two-step method is large agglomerations, whereas single-step method has limited agglomerations. The single-step method has the

advantages in terms of controlling the particle size, reducing the particles agglomeration, and producing nanofluids containing metallic nanoparticles. The disadvantage is that it is difficult to prepare nanofluids with a high particle volume concentration [4].

The volume concentration is evaluated from the following relation in percentage:

$$\varphi = \frac{\text{volume of nanoparticle}}{\text{volume of nanoparticle} + \text{volume of water}} \times 100 \quad (1)$$

or

$$\varphi = \frac{(m/\rho)_{\text{nanoparticle}}}{(m/\rho)_{\text{nanoparticle}} + (m/\rho)_{\text{water}}} \times 100 \quad (2)$$

Due to difficulties of thermal conductivity measurement, it is estimated by the following equation:

$$K_{nf} = K_f \left[\frac{2 + K_{pf} + 2\varphi(K_{pf} - 1)}{2 + K_{pf} - \varphi(K_{pf} - 1)} \right] \quad (3)$$

where

$$K_{pf} = \frac{K_p}{K_f} \quad (4)$$

In addition, thermal conductivity measurement techniques for nanofluids are transient hot-wire technique, transient plane source, thermal constant analyzer technique, thermal comparator, steady-state parallel-plate method, cylindrical cell method, temperature oscillation technique, 3ω method, and laser flash method.

3.2 The effect of nanofluid on heat transfer in a horizontal pipe

The enhancement of the distilled water heat transfer characteristics and the metal oxide nanofluid (ferrofluid)-type (Fe_3O_4) nanoparticles of average diameter

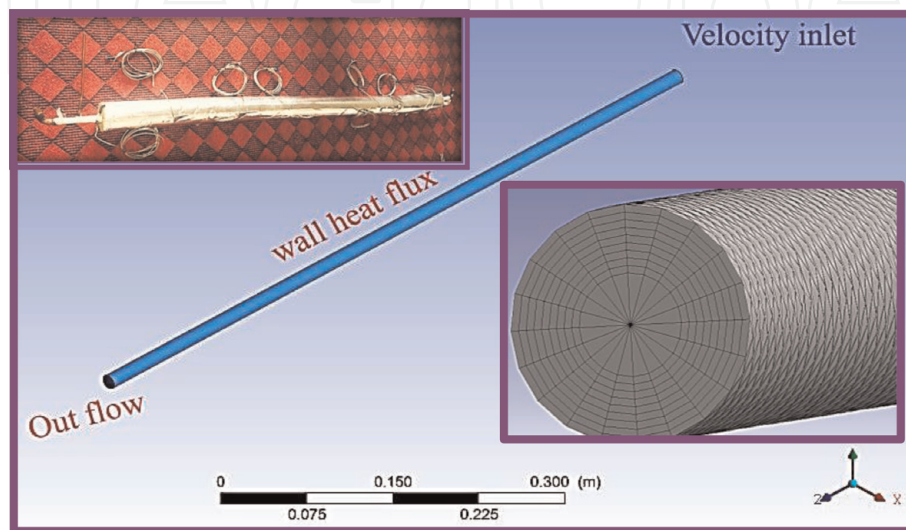


Figure 4. Geometry shape (experimental and numerical) and mesh generated.

(80 nm) with distilled water at concentrations (ϕ) of 0.3, 0.6, and 0.9% by volume in a horizontal pipe have been studied experimentally and numerically [1]. All tests are conducted with the Reynolds number range of 2900–9820 and uniform heat flux 11,262–19,562 W/m². The numerical treatment of the present problem is based on the finite volume technique using commercial CFD software. The system geometry shown in **Figure 4** consists of a copper tube with a diameter of 1.4 cm and a length of 150 cm length. The fluid flows in the tube and is subjected to a uniform heat flux. The number of mesh element in this study is 305,492.

Figure 5 shows the comparison between numerical and experimental results for water and ferrofluid with volume concentration (0 (water), 0.3, 0.6, and 0.9%). An agreement between the results was noticed, and the maximum division was 25, 29, 19, and 7% for nanofluid concentrations of 0, 0.3, 0.6, and 0.9%, respectively. This division could be related to the losses associated with the experimental part which are not taken into account theoretically, and one deals with it as a single-phase flow. However, both results have the same behavior. **Figure 6** shows the contours of temperature at the positions $Z = 0, 0.22, 0.44, 0.66, 0.88, 1.1, 1.32,$ and 0.15 m for a volume concentration of 0.6% and $Re = 5890$. Such contours of temperature manifest increase in temperatures with decreasing ferrofluid concentration or with decreasing velocity.

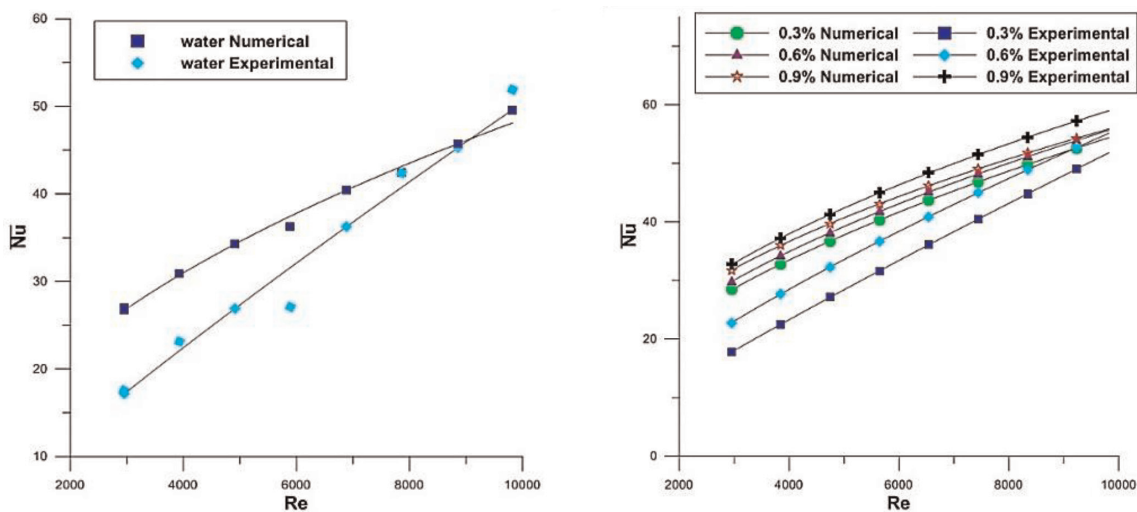


Figure 5.
 Comparison of numerical and experimental results for distilled water and ferrofluid.

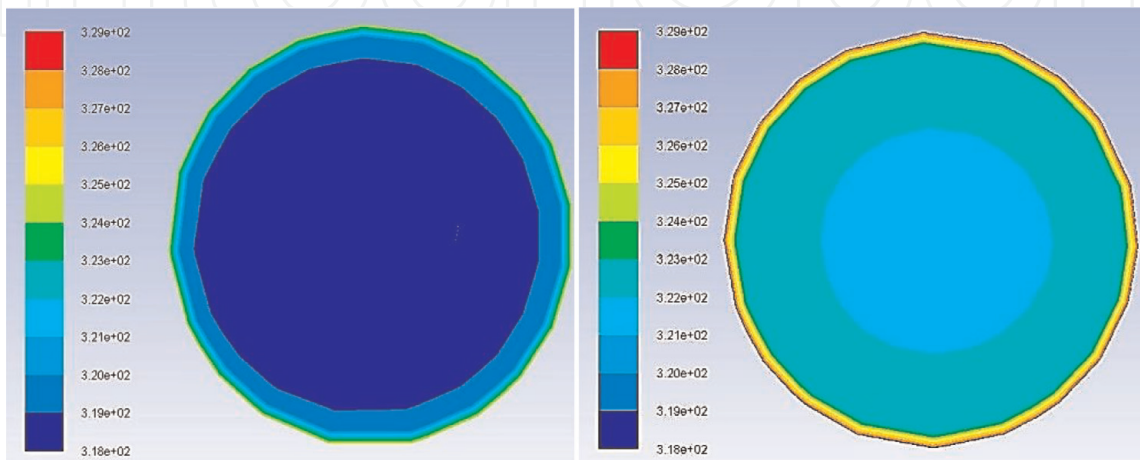


Figure 6.
 Temperature contours in K at locations of $Z = 0.22$ m (left) and 1.32 m (right) along the test section for ferrofluid of volume concentration = 0.6% with $Re = 5890$.

3.3 One- and two-way interaction study of nanofluid characteristics in a finned tube with twisted tape

This section presents an experimental and numerical study to investigate the improvement of the heat transfer and the interaction in a circular finned tube by utilizing one metal oxide [γ - Al_2O_3 (20 nm)]/distilled water nanofluid as a coolant with a typical twisted tape having a twist ratio (TR) of 1.85 [5]. The studied concentrations of nanofluids are $\phi = 0, 3,$ and 5% by volume under laminar and turbulent flow conditions. The study includes constructing a test section that consists of aluminum tube of 1.5 m long, with internal and external diameters of 22 and 32 mm, respectively; see **Figure 7**. The coolant flows through the inner pipe under laminar

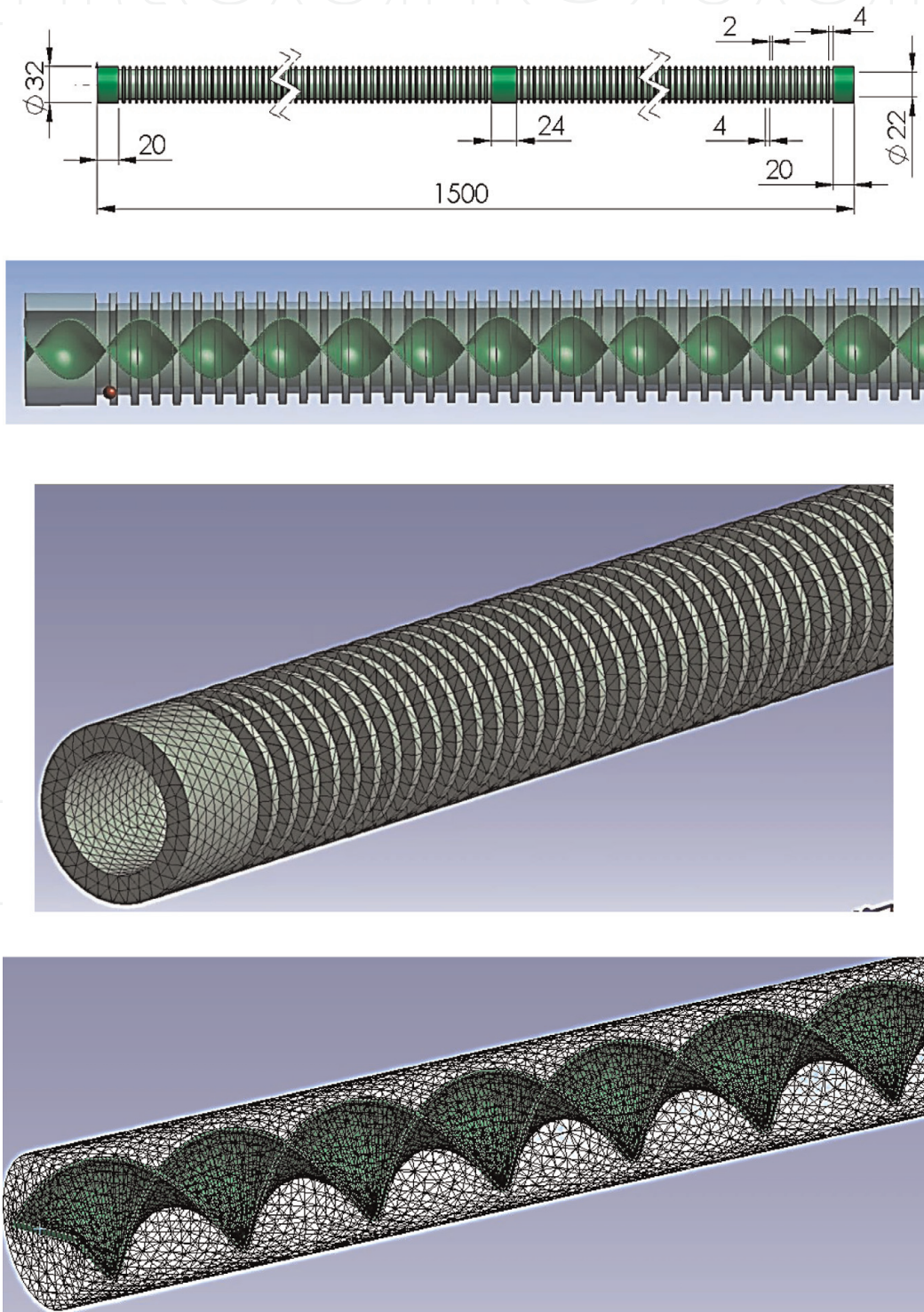


Figure 7. Physical geometry of finned tube (all dimensions in mm), geometry of twisted tape inside a finned tube insert, and meshing geometry.

flow ($678 \geq Re \geq 2033$) and turbulent flow ($3390 \geq Re \geq 10,172$) regime with a constant inlet temperature of 60°C . Because of the complexity of twisted tape configurations and the one- and two-way fluid-structure interaction (FSI), it is impossible to determine an analytical solution of the governing equations for the practical configuration. The numerical simulations permit the intricate geometry analysis of the domain flow and the interaction by multiphysics systems coupling. Therefore, the commercial software of the finite volume numerical methods have been used to solve those equations and to study the interaction pattern of the fluid-heat-structure among fluid flow, typical twisted tape insert, and the finned tube having multidegrees of freedom flow-induced vibration for free and forced vibration.

The mathematical equations utilized for describing the fluid flow are continuity and momentum equations that characterize the conservation of mass and momentum. In addition, the momentum equations are recognized as the Navier-Stokes equations. For flows including heat transfer, another group of equations is needed for describing the energy conservation. Continuity equation is derived via employing the mass conservation principle to a small differential fluid volume. In the Cartesian coordinates, three equations with the following forms are determined. For laminar flow, the continuity, momentum, and energy equations are:

$$\frac{\partial u}{\partial x} + \frac{\partial v}{\partial y} + \frac{\partial w}{\partial z} = 0 \quad (5)$$

$$\rho_{nf} \left(u \frac{\partial u}{\partial x} + v \frac{\partial u}{\partial y} + w \frac{\partial u}{\partial z} \right) = -\frac{\partial p}{\partial x} + \mu_{nf} \left(\frac{\partial^2 u}{\partial x^2} + \frac{\partial^2 u}{\partial y^2} + \frac{\partial^2 u}{\partial z^2} \right) \quad (6)$$

$$\rho_{nf} \left(u \frac{\partial v}{\partial x} + v \frac{\partial v}{\partial y} + w \frac{\partial v}{\partial z} \right) = -\frac{\partial p}{\partial y} + \mu_{nf} \left(\frac{\partial^2 v}{\partial x^2} + \frac{\partial^2 v}{\partial y^2} + \frac{\partial^2 v}{\partial z^2} \right) \quad (7)$$

$$\rho_{nf} \left(u \frac{\partial w}{\partial x} + v \frac{\partial w}{\partial y} + w \frac{\partial w}{\partial z} \right) = -\frac{\partial p}{\partial z} + \mu_{nf} \left(\frac{\partial^2 w}{\partial x^2} + \frac{\partial^2 w}{\partial y^2} + \frac{\partial^2 w}{\partial z^2} \right) \quad (8)$$

$$(\rho C_p)_{nf} \left(u \frac{\partial T_{nf}}{\partial x} + v \frac{\partial T_{nf}}{\partial y} + w \frac{\partial T_{nf}}{\partial z} \right) = K_{nf} \left(\frac{\partial^2 T_{nf}}{\partial x^2} + \frac{\partial^2 T_{nf}}{\partial y^2} + \frac{\partial^2 T_{nf}}{\partial z^2} \right) \quad (9)$$

For turbulent flow, the continuity, momentum, and energy equations and turbulence kinetic energy (k) and its dissipation rate (ϵ) are:

$$\frac{\partial \bar{u}}{\partial x} + \frac{\partial \bar{v}}{\partial y} + \frac{\partial \bar{w}}{\partial z} = 0 \quad (10)$$

$$\begin{aligned} & \left(\bar{u} \frac{\partial \bar{u}}{\partial x} + \bar{v} \frac{\partial \bar{u}}{\partial y} + \bar{w} \frac{\partial \bar{u}}{\partial z} \right) + \left(\frac{\partial}{\partial x} (\overline{u'^2}) + \frac{\partial}{\partial y} (\overline{u'v'}) + \frac{\partial}{\partial z} (\overline{u'w'}) \right) \\ & = -\frac{1}{\rho_{nf}} \frac{\partial p}{\partial x} + \gamma \nabla^2 \bar{u} \end{aligned} \quad (11)$$

$$\begin{aligned} & \left(\bar{u} \frac{\partial \bar{v}}{\partial x} + \bar{v} \frac{\partial \bar{v}}{\partial y} + \bar{w} \frac{\partial \bar{v}}{\partial z} \right) + \left(\frac{\partial}{\partial x} (\overline{u'v'}) + \frac{\partial}{\partial y} (\overline{v'^2}) + \frac{\partial}{\partial z} (\overline{v'w'}) \right) \\ & = -\frac{1}{\rho_{nf}} \frac{\partial p}{\partial y} + \gamma \nabla^2 \bar{v} \end{aligned} \quad (12)$$

$$\begin{aligned} & \left(\bar{u} \frac{\partial \bar{w}}{\partial x} + \bar{v} \frac{\partial \bar{w}}{\partial y} + \bar{w} \frac{\partial \bar{w}}{\partial z} \right) + \left(\frac{\partial}{\partial x} (\overline{u'w'}) + \frac{\partial}{\partial y} (\overline{v'w'}) + \frac{\partial}{\partial z} (\overline{w'^2}) \right) \\ & = -\frac{1}{\rho_{nf}} \frac{\partial p}{\partial z} + \gamma \nabla^2 \bar{w} \end{aligned} \quad (13)$$

$$\left(\bar{u} \frac{\partial \bar{T}_{nf}}{\partial x} + \bar{v} \frac{\partial \bar{T}_{nf}}{\partial y} + \bar{w} \frac{\partial \bar{T}_{nf}}{\partial z} \right) = \alpha \nabla^2 \bar{T}_{nf} + \left(-\frac{\partial}{\partial x} (\overline{u'T'_{nf}}) - \frac{\partial}{\partial y} (\overline{v'T'_{nf}}) - \frac{\partial}{\partial z} (\overline{w'T'_{nf}}) \right) \quad (14)$$

$$\frac{\partial}{\partial t} (\rho_{nf} k) + \frac{\partial}{\partial x_i} (\rho_{nf} k u_i) = \frac{\partial}{\partial x_j} \left[\left(\mu + \frac{\mu_t}{\sigma_k} \right) \frac{\partial k}{\partial x_j} \right] + G_k + G_b - \rho_{nf} \varepsilon - Y_M + S_k \quad (15)$$

$$\frac{\partial}{\partial t} (\rho_{nf} \varepsilon) + \frac{\partial}{\partial x_i} (\rho_{nf} \varepsilon u_i) = \frac{\partial}{\partial x_j} \left[\left(\mu + \frac{\mu_t}{\sigma_k} \right) \frac{\partial \varepsilon}{\partial x_j} \right] + C_{1\varepsilon} \frac{\varepsilon}{k} (G_k + C_{3\varepsilon} G_b) - C_{2\varepsilon} \frac{\varepsilon^2}{k} + S_\varepsilon \quad (16)$$

Grid independence test is carried out to obtain the most suitable computational grid for which a finer grid provides the similar outputs with the initial one, and the outputs do not vary as grid becomes finer. The checking procedure, either the solution is grid independent or not, is to generate a grid with many cells for comparing the solutions of both models. The tests of grid refinement for Nusselt number explain that the grid size of almost 2 million cells provides a sufficient accuracy and resolution to be adopted as the standard for all cases. The grid independence test performed for typical twist tape with TR = 1.85 configuration is shown in **Figure 8**.

The analysis of fluid-structure interaction (FSI) is an instant of a multiphysics problem, where the interaction between two dissimilar analyses is taken into consideration. This analysis includes conducting a structural analysis taking into consideration the interaction with the corresponding fluid analysis. The interaction between both analyses distinctively occurs at the model solution boundary (the

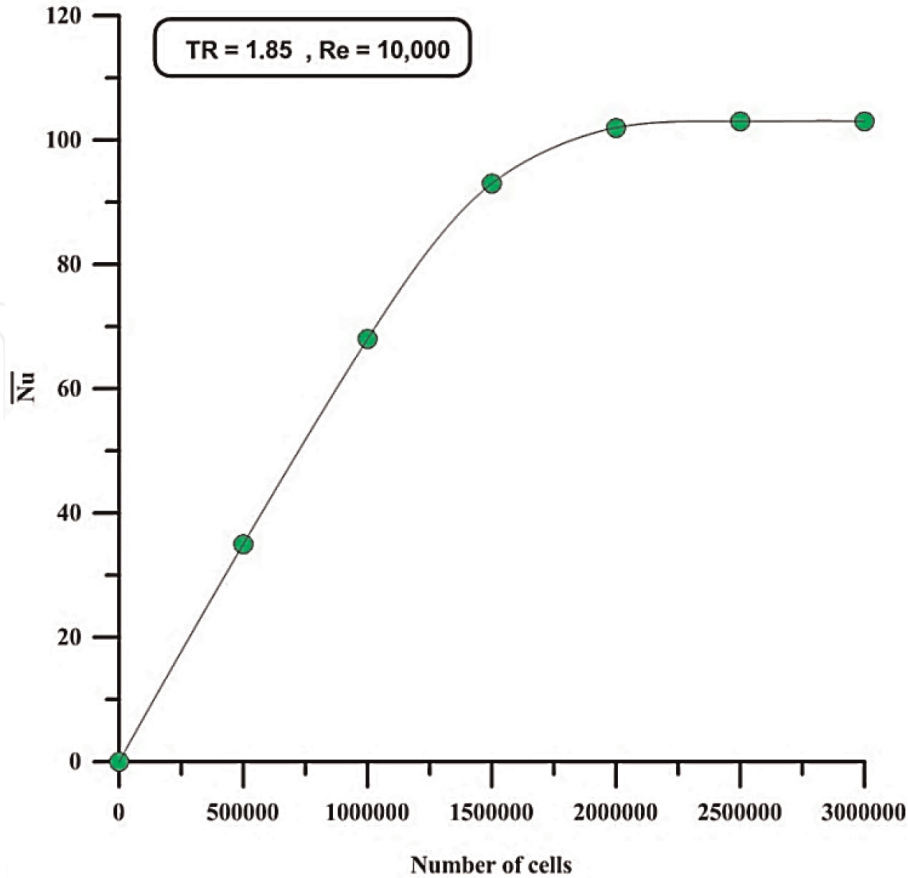


Figure 8.
The grid-independent solution test for typical twisted tape.

fluid-structure interface), where the outputs of one analysis are passed to the other one as a load. There are two different fluid-structure interaction approaches that can be used, depending on the physical nature of the interaction. The multiphysics problems are too hard to solve via the analytical approaches. Accordingly, they must be solved either via employing experiments or numerical simulations. The progressed methods and the existence of the reckoned commercial software in both CFD and computational structural mechanics (CSM) have made such numerical simulation possible. There are two dissimilar methods to solve the problems of FSI utilizing such software: the monolithic method and the partitioned method. In one-way coupled FSI, the results (forces) from the fluid analysis at the fluid-structure interface are applied as a load to the structural analysis. The boundary displacement from the structure is not passed back to the fluid analysis. The assumption is that the deformation of the structure is small, having insignificant effect on the fluid flow prediction. This allows the fluid analysis and structure analysis to be run independently. This technique will be used for the theoretical analysis. In the two-way coupled FSI, the structural analysis results are conveyed to the fluid analysis as a load. In a similar way, the fluid analysis results are passed back to the structural analysis as a load. For instance, the fluid pressure at the boundary can be applied as a load on the structural analysis, and the resulted displacement, velocity, or acceleration determined in the structural simulation could be passed on as a load to the fluid analysis. The analysis will carry on till the whole equilibrium (convergence) is attained between the fluid flow solution and the structural solution.

The simulated values of average Nusselt number are compared with the experimental results, as shown in **Figure 9**. The computed values agree with the experimental data within ± 13 and $\pm 12\%$ for laminar and turbulent flow, respectively. The simulated friction factors along the tube against the Reynolds no. are also compared to those determined from the experiments. It's noticed that the simulated data are matching with the experimental data within $\pm 11\%$ for the average Nusselt no. and $\pm 9\%$ for the friction factor, respectively. However, both results have the same behavior, and the differences are with acceptable values. **Figure 10** shows the velocity vector at location of $Z = 0.5$ m along the test section. A secondary flow is created, and a rotational movement is noted along the tube, and this will enhance the heat transfer within the tube.

Figure 11 elucidates the 3D view for the distribution of static temperature along the test section at the midplane (environment and tube) for a nanofluid having a 3%

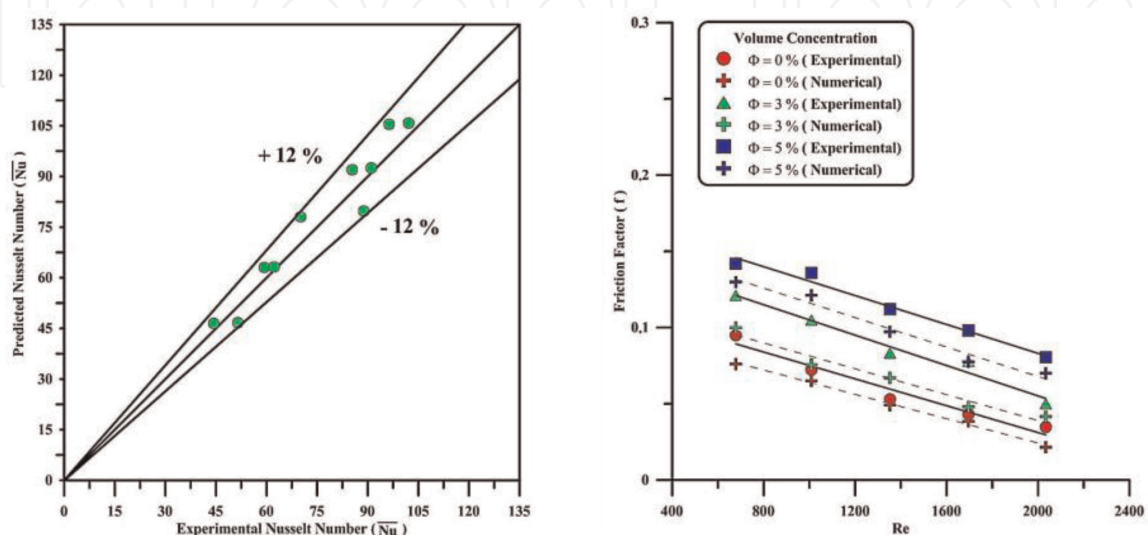


Figure 9.
 Comparison of experimental and predicted \bar{Nu} for turbulent flow and for Re and f for laminar flow.

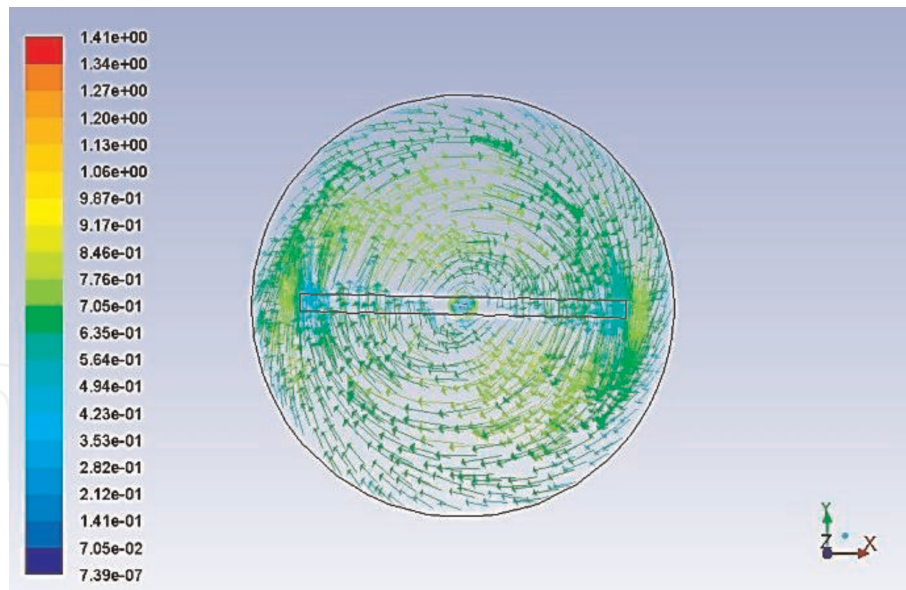


Figure 10.
Velocity vectors in m/s at $Re = 10,172$ for nanofluid ($\phi = 3\%$) at $Z = 0.5$ m.

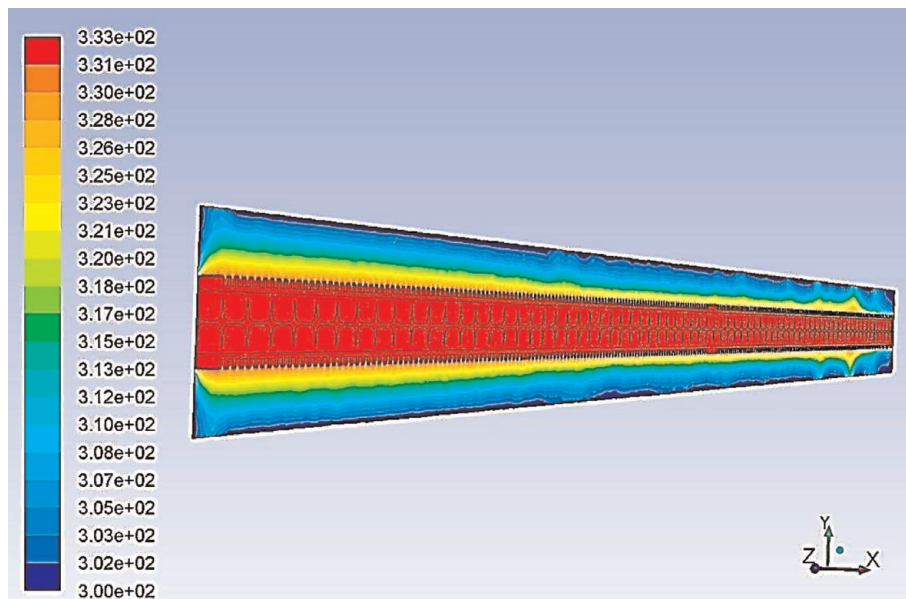


Figure 11.
Temperature distribution along the test section for $\phi = 3\%$.

volume concentration and a Reynolds no. equal to 5086 for a turbulent flow.

Figure 12 shows the test section deformation calculated using static structural-mechanical is a solution processing model, under the influence of enlarging its value (1.8×10^3 autoscale). The maximum deformation occurs at the beginning of the tube in all models because of the high temperature concentration at this region. From this figure, one can see that the total deformation decreases as the volume concentration and the mass flow rate increase due to the frequency effect, which is decreased with the increase in nanoparticle mass.

Figure 13 highlights the 3D view for the twisted tape with the velocity vector along a focused distance of the test section for a nanofluid having a 3% volume concentration. In this figure, one can see that the vector magnitude and direction change at different periods of time due to effect of the twisted tape deformation, which is much higher than that of the tube, resulted from thermal expansion (elongation), fluid pressure effect, and reaction force on it.

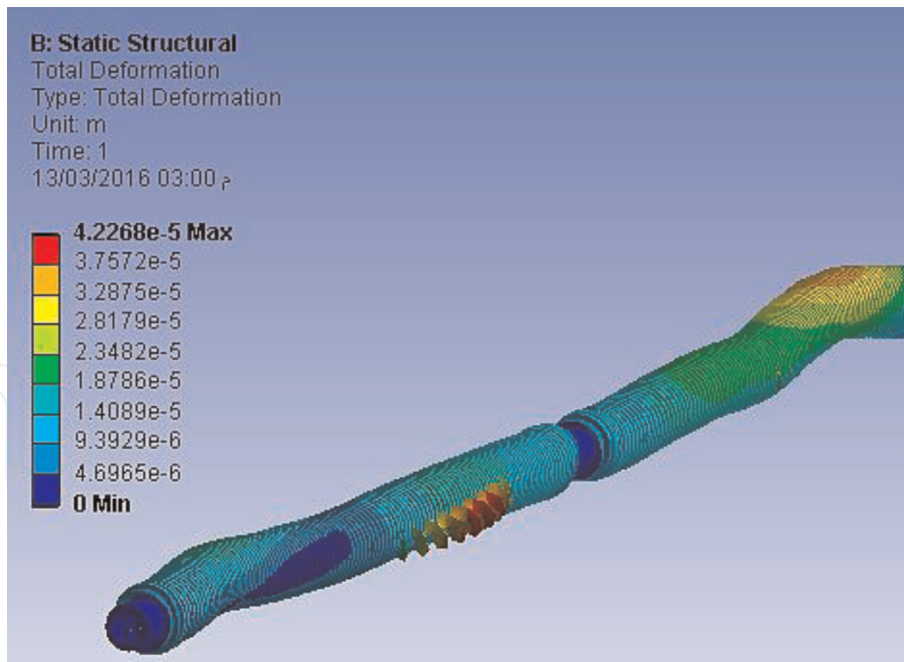


Figure 12.
Total deformation from one-way interaction for $Re = 10,172$ and $\varphi = 5\%$.

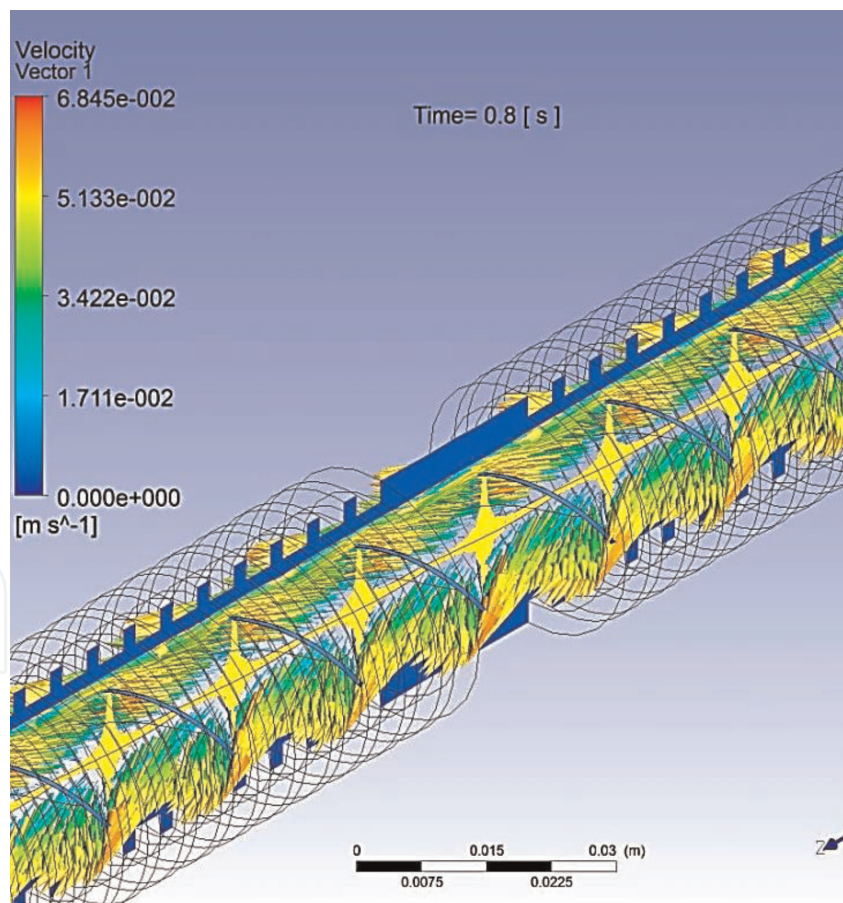


Figure 13.
Velocity vectors for two periods at $Re = 678$ and $\varphi = 3\%$ and $T_2 = 0.8$ s.

4. Selected topics in medicine and biology

During the previous decades, there has been a significant raise in the use of quantitative techniques for studying the physiological regimes. Recent methods for

conducting the physiological measurements are being steadily evolved and used, and there has been a relevant rise in the techniques that exist for analyzing and interpreting the data of experiment. Increasingly, such methods are obtaining their way within the physiological studies and in the related studies in clinical sciences and medicine. A supplementary driver for the whole of this is, certainly, the existence of further computing power. Utilizing the whole of these gathered is causing an increment in the use of mathematical modeling approaches in the physiological studies. The further use of modeling and dynamic regime analysis provides advantages for the biomedical engineering, governing and regime science, and physiology. The proper application of mathematical models provides numerous potential advantages for the physiologist. Such models offer a brief explanation of intricate dynamic operations, indicating the methods, in which the enhanced experimental design can be performed, and empowering the hypotheses regarding the physiological structure to be examined. Further to that, they permit the estimates to be done for the factors (physiological quantities) that are in different way not straightforward able to be reached to measurement. Despite firstly the most modeling uses have been in the fields of medical and physiological investigation, they are presently further being utilized as assistances in diagnosing and treating the disease [6]. The biomedical engineering (BME) is an engineering branch involved with solving problems in the biology and the medicine. Biomedical engineers use principles, methods, and approaches drawn from the more traditional branches of electrical, mechanical, chemical, material, and computer engineering to solve this wide range of problems. They use them with other fundamentals to the problems in the fields of life sciences and healthcare, i.e., this engineer must also be familiarized with the biological ideas of physiology and anatomy at the cellular, molecular, and regime levels. Practicing the healthcare needs the familiarization with the nervous system, cardiovascular regime, circulation, respiration, body fluids, and kidneys. The biomedical engineering field is expanding fast. The biomedical engineers will take a big role in the investigation in the life sciences and device evolution for the adequate healthcare delivery. The biomedical engineering scope ranges from the bionanotechnology to the assisting instruments, from the cellular and molecular engineering to the robotics of surgery, and from the neuromuscular regimes to the synthetic lungs. The ideas introduced in this context will assist the biomedical engineers to operate in such variant field [7].

4.1 Dentistry analysis

Dental scientists are making increased usage of computational methods, particularly in situations where the experimental procedures fail to give proper answers. An experimental procedure may explain the maximum load of a tooth failure, but it cannot give an accepted reply around the failure evolution mechanism. Dentistry analysis is done in many ways, such as stress analysis, fluid mechanics and dynamic analysis, thermal analysis, restorative material analysis, and so on. The structure of the normal tooth conveys the loads of the external biting via the enamel within the dentin. Since the teeth aren't stiff structures, so they subject to deformation (strain) during the usual loading. The focused external loads are spread over a big internal volume of the tooth structure, and thus the local stresses are less. Within such operation, a little quantity of the dentin deformation may take place that causes the tooth bending. If a load is exerted, the structure is subject to a deformation since its bonds are sheared, stretched, or compressed. As the loading progresses, this structure will deform. Firstly, such deformation (strain) is totally a reversible elastic strain. However, the incremented loading eventually makes also certain irreversible strain (plastic strain) that results in a fixed deformation. The

onset of the plastic strain point is named the elastic limit (proportional limit, or yield point). This point is exhibited on the stress-strain curve at the point, where the straight line begins to be curved. Thus, progress of the plastic strain ultimately results in a failure via fracture. The largest stress prior to fracture is the maximum strength, and the whole tensile strain (plastic) at the fracture is named the elongation. **Figure 14** shows the sound and restored teeth models with finite element mesh. Since the enamel is of greater stiffness than that of the dentin, it will take most of the applied load and distributes it all over the dentin in a uniform manner. In this case, only small values of stress will reach the dentin. Whereas, in **Figure 15A**, Young's modulus values of the enamel are assumed to be high, the load is applied at the tip of the buccal cusp. The enamel is acting here as a stress distributor, where the stress would transfer in a shape very similar to the stressed enamel. Moreover, when Young's modulus value of the enamel is low, the stress tunnels through the enamel in a sharp manner, reaching the dentin, which is assumed to be of higher Young's modulus value (**Figure 15B**). Then, the dentin in turn would act as a stress distributor when transmitting it to the following parts and the pulp [8].

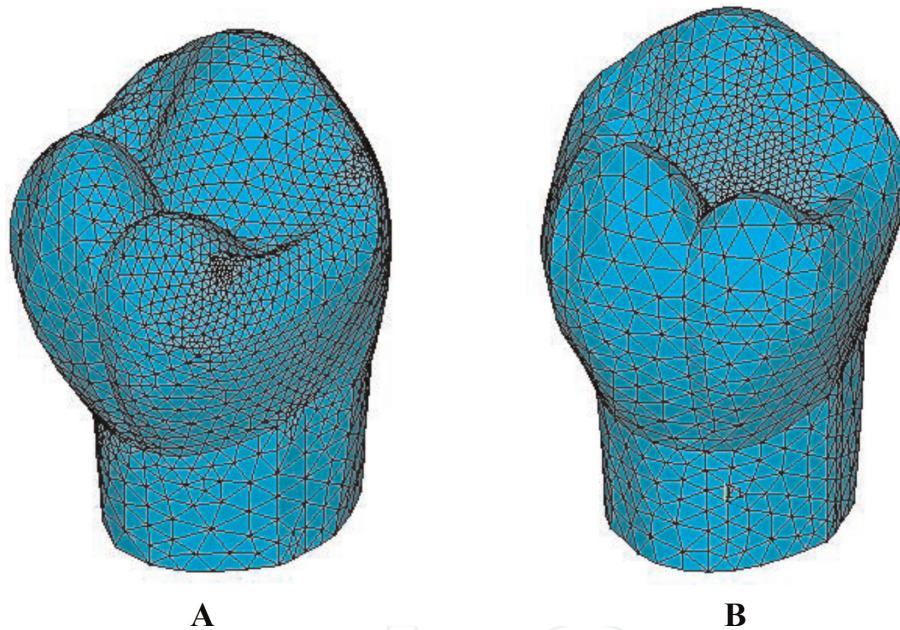


Figure 14.
Mesh of (A) sound model and (B) restored model.

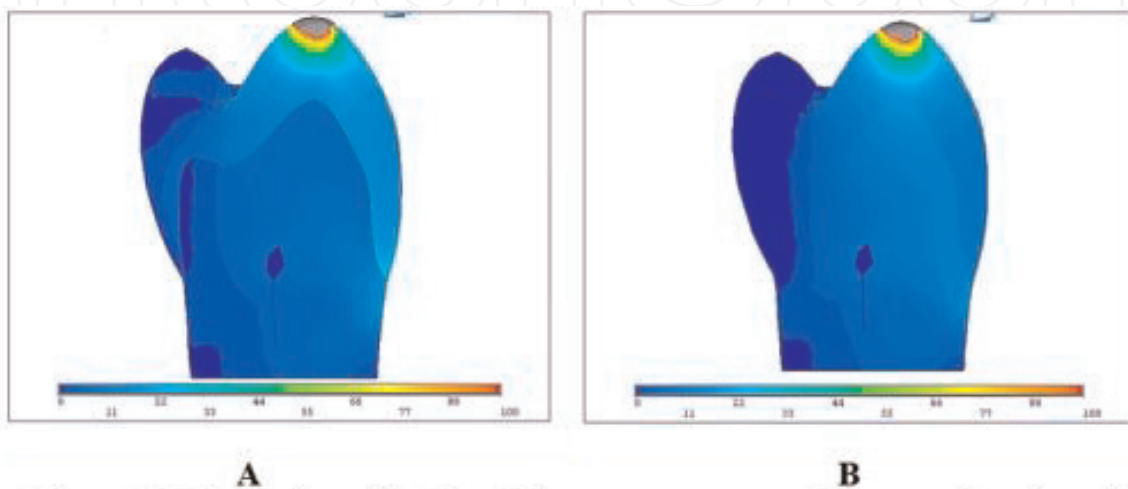


Figure 15.
Distribution of the von Mises stress contour of the sound tooth model subjected to loading case.

4.2 Contaminant degradation

One of the specific bioremediation mechanisms is the contaminant degradation in the soil via the plant enzymes that are exuded from the roots. For the soil that is contaminated by petroleum, the result of bioremediation is suggested to be depended upon the degrading microorganism stimulation in the rhizosphere, named rhizodegradation or phytostimulation. The biodegradation is commonly a slow operation owing to the contaminant's hydrophobic nature and the resulted bioavailability limitations. The petroleum hydrocarbons, like diesel with the n-alkane markers that range in size from C8 to C25, are mostly decreased organic molecules that can work as a carbon origin and electron donor for the microorganisms, for supporting the microbial metabolism. The hydrocarbon biodegradation reduces with the raise of the molecular weight. Microorganisms are able to degrade the hydrocarbons with a broad range of n-alkanes between C10 and C35, among which C14–C19 are desired. Beneath the anaerobic circumstances, the electron acceptors other than O₂ are utilized for the microbial respiration and through such operation; hydrocarbons are oxidized to the intermediate molecules and finally to CO₂, whereas the terminal electron acceptors are decreased. Rhizobacteria (RB) are characterized as the bacteria that live in the surrounding area of the root or on the surface of the root. The hydrocarbon degradation is enhanced via a rhizosphere influence with plants that exude the organic constituents throughout their roots, affecting the variety, abundance, or the ability of potential hydrocarbon to degrade the microorganisms in the region that surrounds the roots. The roots provide suitable attachment locations for the microorganisms and also provide the nutrients in the shape of exudates composing of organic acids and amino acids, sugars, enzymes, and intricate carbohydrates. Moreover, the root exudates from plants do help to degrade the toxic organic chemicals and acts as substrates for the soil microorganisms to increase the biodegradation rate of the organic contaminants. The hydrocarbon-contaminated soil biodegradation that exploits the capability of microorganisms for degrading and/or detoxifying the organic contamination has been built as an adequate, versatile, economic, and environmentally a good processing for the kerosene-contaminated soils. The microorganisms make biosurfactant being plentiful in nature; they hinder the water (groundwater, seawater, and freshwater) and the land (sediment, sludge, and soil). Additionally, they can be obtained in the utmost surroundings (e.g., reservoirs of oil) and prosper at a broad range of salinity, temperatures, and pH values. Nevertheless, the microbial communities of hydrocarbon-degrading abide the highly proper ambient for a broad capability for the production of biosurfactant. The hydrocarbon-degrading bacterial populations are, in general, prevailed via a few major genera, including *Sphingomonas*, *Bacillus*, *Actinobacteria* in sediments and soils, *Pseudomonas* and *Klebsiella*, and *Halomonas*, *Alcanivorax*, *Acinetobacter*, and *Pseudoalteromonas* in the marine ecosystems. It has been documented that 2–3% of the screened populations within the uncontaminated soils are microorganisms that produce biosurfactant. That raises to 25% in the polluted soils. From the other side, the methods of enrichment culture, specifically for the hydrocarbon-degrading bacteria, may result a greater detection of the biosurfactant makers with estimates till 80%. The biosurfactants made via microorganisms are divided into two various classes depending upon their chemical composition: like the surface-active agents with less molecular weight named biosurfactants and the biosurfactants with more molecular weight denoted as bioemulsifiers.

4.3 Wastewater treatment

One of the multiphase flow applications is the three-phase fluidized bed (gas-liquid-solid fluidized bed) which has appeared recently as one of the major

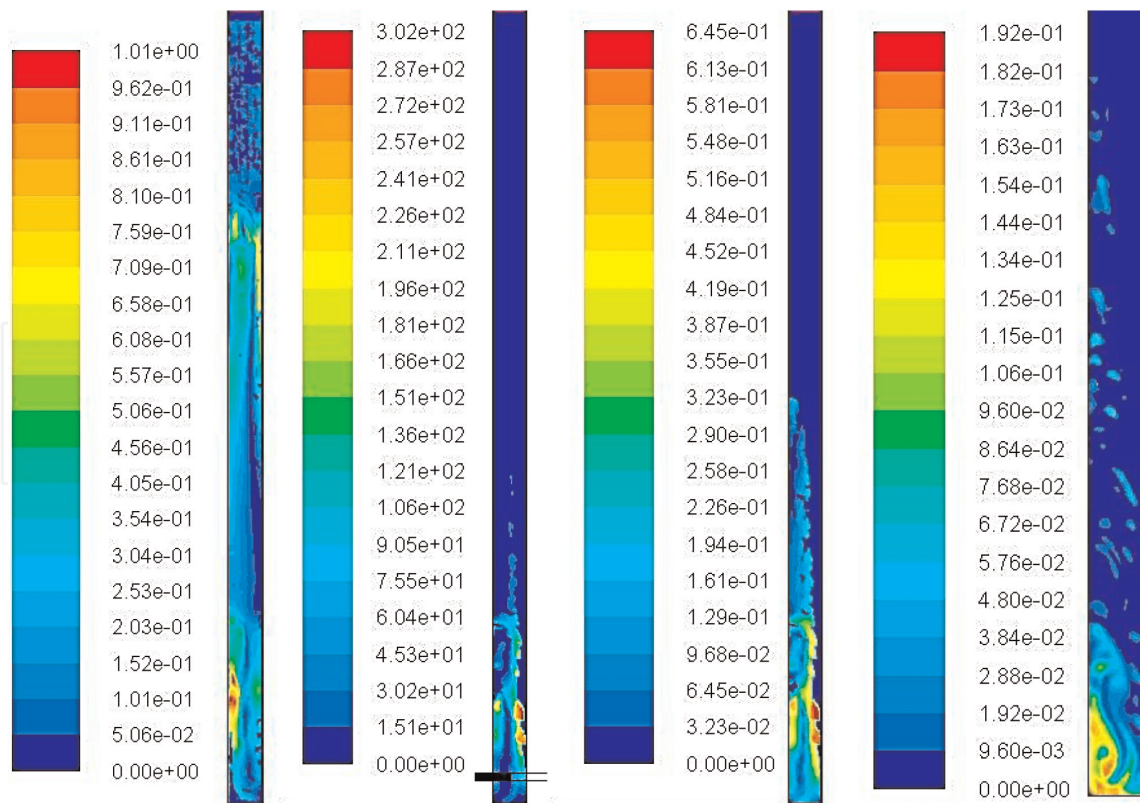


Figure 16. Contours of velocity magnitude for air in m/s, contours of dynamic pressure for solid particles in Pascal, contours of velocity magnitude for solid particles in m/s, and contours of volume fraction for solid particles, respectively.

promising instruments for the three-phase process. This instrument is of important industrial significance as proofed from its broad use in the chemical, biochemical, and petrochemical treatment. The fluidized beds work in numerous aims in the industry, like promoting the catalytic and non-catalytic reactions. Three-phase fluidized beds have been used adequately in numerous industrial operations, like in the H₂-oil operation for the residual oil hydrogenation and hydrodesulfurization; H-coal operation for the coal liquefaction; Fischer-Tropsch operation; bio-oxidation process for wastewater treatment; biotechnological operations, such as pharmaceuticals and mineral industries; fermentation and aerobic wastewater processing; and so on. One of the recent biotechnological process applications is the study of three-phase fluidized beds for dried algae such as chlorella after they are mixed, crushed, dried, and immobilized to us as the solid phase. The liquid phase is the water, and the gas phase is the air. **Figure 16** represents (from left to right) the contours of velocity magnitude for air in m/s at time = 3 s, contours of dynamic pressure for solid particles in Pascal at time = 3 s, contours of velocity magnitude for solid particles in m/s at time = 3 s, and contours of volume fraction for solid particles at time = 3 s, respectively.

5. Conclusion

Nanofluids, as mentioned earlier, are prepared from suspending nanoparticles into dilute liquid. The thermal behavior of nanofluids may offer a huge invention for heat transfer. Too many applications are in field of nanofluidics: transportation, electronics cooling, nuclear systems cooling, boiler flue gas temperature reduction, energy efficient cooling, heating of buildings without increased pumping power in heating, ventilation and air conditioning, heat exchangers, biomedical industry, for example, traditional cancer treatment method, kill cancers cells, drugs radiation

without damaging, cool the brain, safer surgery, heat pipes, fuel cell, solar water heating, domestic refrigerator, diesel combustion, thermal storage, etc. Solving CFD problem usually consists of four components: geometry and grid generation, setting up a physical model, solving it, and post-processing the computer data. The created geometry and grid are generated, the set problem is computed, and the way acquired data is presented is very well known. Precise theory is available. Mathematical modeling is now widely applied in physiology and medicine to support the life scientist and clinical worker. Mathematical modeling finds application in medical research, in education, and in supporting clinical practice. The use of models can, for example, yield quantitative insights into the manner in which physiological systems are controlled. In the educational setting, medical students can use computer model simulation to explore the dynamic effects of pathophysiological processes or of drug therapy. In the clinical arena, mathematical models can enable estimates to be made of physiological parameters that are not directly measurable—useful for example in diagnosis, as well as enabling predictions to be made as to how changes in drug therapy will impact on variables of clinical importance such as blood pressure or blood glucose concentration.

Acknowledgements

The authors would like to thank the University of Technology and Al-Mustaqbal University College for the support in the present work.

Nomenclature

Cp_{nf}	specific heat of nanofluid at constant pressure (kJ/kg.K)
k_{nf}	thermal conductivity of the nanofluid (W/m.K)
p	pressure (N/m ²)
T	temperature (°C)
u, v, w	velocity component in Cartesian coordinate (m/s)
x, y, z	Cartesian coordinate (m)

Greek symbols

ε	dissipation rate (1/s)
k	turbulent kinetic energy (m ² /s ²)
ρ_{nf}	density of the nanofluid (kg/m ³)
φ	volume fraction (Vol.%)
∇	represents the partial derivative of a quantity with respect to all directions in the chosen coordinate system (—)

Subscripts

i, j, k	tenser indices
nf	nanofluid

Superscripts

$()'$	fluctuation component
--------	-----------------------

IntechOpen

Author details


Laith Jafer Habeeb^{1*} and Hasan Shakir Majdi²

1 Training and Workshops Center, University of Technology, Baghdad, Iraq

2 Al-Mustaqbal University College, Babylon, Hillah, Iraq

*Address all correspondence to: laithhabeeb1974@gmail.com

IntechOpen

© 2019 The Author(s). Licensee IntechOpen. This chapter is distributed under the terms of the Creative Commons Attribution License (<http://creativecommons.org/licenses/by/3.0>), which permits unrestricted use, distribution, and reproduction in any medium, provided the original work is properly cited. 

References

[1] Asker AH. The effect of magnetic field with nanofluid on heat transfer in a horizontal pipe [thesis]. Baghdad-Iraq: Mechanical Engineering Department, University of Technology; 2016

[2] Versteeg HK, Malalasekera W. Introduction to Computational Fluid: The Finite Volume Method. England: Longman Scientific & Technical; 1996

[3] Cheng L. Nanofluid Heat Transfer Technologies. Recent Patents on Engineering. Bentham Science Publishers; Vol. 3, Number 1, 2009. pp. 1-7(7)

[4] Yu W, Xie H. A review on nanofluids: Preparation stability mechanisms, and applications. Journal of Nanomaterials. 2012;2012:1-17. Article ID 435873

[5] Magel BM. One and two-way interaction study of nanofluid characteristics in a finned tube with twisted tape [thesis]. Baghdad-Iraq: Mechanical Engineering Department, Faculty of Engineering, Al-Mustansiriayah University; 2016

[6] Cobelli C, Carson E. Introduction to Modeling in Physiology and Medicine. 1st ed. Amsterdam: Academic Press is an imprint of Elsevier; 2008

[7] Dunn SM, Constantinides A, Moghe PV. Numerical Methods in Biomedical Engineering. Amsterdam: Academic Press is an imprint of Elsevier; 2006

[8] Abdul-Khaliq Hussain W. Stresses analysis of sound and restored teeth [thesis]. Baghdad-Iraq: Department of Applied Sciences, University of Technology; 2007